

論文2001-38SD-12-5

# $\lambda/4$ 천이영역을 갖는 광 DFB도파로의 해석적 분석법

## (A Simple Analytic Method of Optical DFB Waveguides with Quarter-Wavelength Shifted Region)

金俊煥\*, 扈光春\*\*

(June-Hwan Kim and Kwang-Chun Ho)

## 요 약

$\lambda/4$  천이영역을 갖는 평면 DFB 도파로의 광학적특성을 분석하였다. 그 도파로의 필터특성과 공진특성을 정확히 분석하기 위하여 Floquet 이론과 Babinet 원리에 기초한 새로운 모드 전송선로 이론을 유도하였다. 수치해석 결과, 본 논문에서 제시한 해석법은  $\lambda/4$  천이영역을 갖는 평면 DFB 도파로의 필터 특성과 공진 특성을 간단히 해석할 수 있는 알고리즘을 제공하며, 다른 근사적 해석법들에서 얻을 수 없는 새로운 물리적 특성을 보여 주었다.

## Abstract

We evaluate the optical characteristics of planar distributed feedback (DFB) waveguides with quarter-wavelength phase-shifter. To analyze explicitly its band-pass and resonance properties, we present and newly develop a modal transmission-line theory (MTLT) based on Floquet's theorem and Babinet's principle. The numerical results reveal that this approach offers a simple and analytic algorithm to analyze either the filtering or the oscillating characteristic of DFB gratings with quarter-wavelength phase-shifter, and has a novel physical insight that may not be achieved in other approximating approaches

## I. Introduction

Kogelnik and Shank<sup>[1]</sup> have proposed distributed-feedback (DFB) guiding structures for the applications of integrated optics. The geometry may act as mirrors or filters operating at optical wavelength, and be

incorporated in most of the optoelectronic devices because of the frequency-selective property applicable to optical communications. The transmission characteristic is really a stop-band filter rather than a pass-band filter.

However, in many applications, the optical transmission system practically requires a channel-dropping function, in which a narrow channel is selected from large spectrum of designed channels. If one spaces two periodic structures by one (or an odd multiple of) quarter wavelength, it is possible to achieve an optical filter served as pass-band transmitter. Furthermore, the DFB grating having a discrete phase-shift region at the center of two DFB gratings generates a single resonance mode while one without phase-shift region has two-mode oscillation property.

\* 正會員, 三星綜合技術院

(Samsung Advanced Institute of Technology)

\*\* 正會員, 漢城大學校 情報通信工學科

(Hansung University, Dept. of Information and Communication Eng.)

\* This research was financially supported by Hansung University in the year of 2001.

接受日字:2000年8月31日, 수정완료일:2001年10月30日

This means the fact that the spacer to keep a track of phase shift will form an effective resonator inside the optical path, and thus affect the device operation.

To acquire and analyze numerically the design parameters suitable to the single mode transmission at long-haul optical communication, many approaches<sup>[2-3]</sup> have claimed themselves capability. One of those candidates used widely is coupled-mode theory (CMT). Although this approach can be applied to more general guiding structures, it becomes too complicated and laborious when carrying out the numerical analysis of configurations cascaded by DFB guides with different grating profiles. On the contrary, the transfer matrix method (TMM), which is a famous candidate of very competitive simplified methods, still gives us an excellent computational algorithm to evaluate the DFB gratings composed by multiple-sections. However, it does not supply the physical insight in detail of modal fields distributing and traveling at the DFB guides with phase-shifter.

One way to overcome those disadvantages is to use such an analogous approach, which is called modal transmission-line theory (MTLT)<sup>[4]</sup> and satisfies the pertinent boundary conditions of Maxwell's equations. To achieve this objective, in Section 2 of this paper we present a simple and newly developed MTLT using Floquet's theorem<sup>[5]</sup> and bisection principle (Babinet's theorem)<sup>[6]</sup> to analyze the optical filtering and oscillating characteristics of phase-shifted DFB guiding profiles. In addition, the oscillating property of a single TE resonance mode is explicitly investigated and discussed in Section 3. Consequently, we give the conclusive remarks in Section 4.

## II. Modal Characteristics of Newly Developed MTLT

### 1. Equivalent Propagation Constant

A quarter-wavelength phase-shifted DFB guide is schematically shown in Fig. 1(a). This device consists of two Bragg gratings separated by a spacer whose length represents exactly half the period of the Bragg

gratings. The substrate layer is composed of a material To determine the design parameters for practical application, we develop a simple and newly developed MTLT based on the equivalent propagation constant

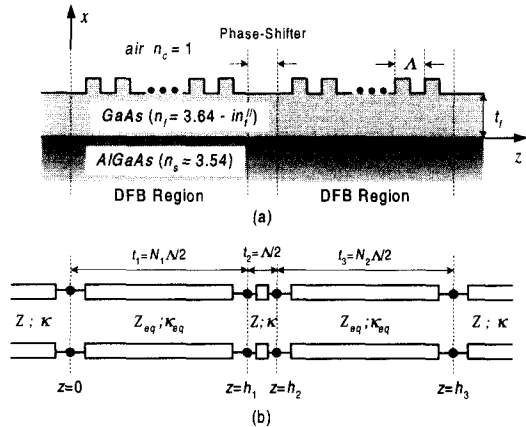


그림 1.  $N$ 개의 격자로 구성된 평면 DFB 전송구조 : (a) 평면구조, (b) 등가 전송선로

Fig. 1. A symmetric DFB guiding structure with a finite number  $N$  of gratings depicted by (a) a plane of geometry, and (b) the equivalent network.

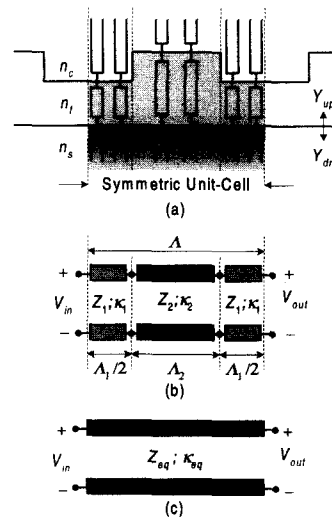


그림 2. 등가전송선로망 : (a) 단위 셀의 각 영역, (b) 대칭 단위셀, (c) Floquet 원리를 만족하는 단위셀.

Fig. 2. Equivalent transmission-line networks (a) for each section of unit-cell, (b) for a symmetric unit-cell, (c) satisfying Floquet's theorem.

$\kappa_{eq}$  and characteristic impedance  $Z_{eq}$ , which describes the modal effect of multi-layered periodic guiding structures. This defined modal representation is then evaluated by conventional transmission-line considerations satisfying the boundary conditions of Maxwell's equations, as depicted in Fig. 1(b). Figure 1(b) shows that the DFB regions with grating length  $L_1 = N_1 \Lambda/2$  and  $L_2 = N_2 \Lambda/2$  can be analogous to transmission-line blocks with the equivalent modal components of periodic guiding structures and the other regions including phase-shifter be replaced by uniform constituent blocks of stratified guides. Thus, the quarter-wavelength phase-shifted DFB guide acts as a transmission-line network with five blocks.

Assuming that a plane wave with operating wavelength  $\lambda = 0.86 \mu\text{m}$  is incident from the left-hand side of guiding structure, we then construct an equivalent transmission-line network for the symmetric unit-cell with input ( $V_{in}$ ) and output ( $V_{out}$ ) terminal voltages describing the amplitudes of the guiding fields, as shown in Fig. 2. From Fig. 2(a) it is easy to understand intuitively that the DFB guide is comprised by a series of symmetric unit-cells with length  $\Lambda = \Lambda_1 + \Lambda_2$ . Consequently, we can determine well the local propagation constants  $\kappa_1$ ,  $\kappa_2$  for each segment having length  $\Lambda_1/2$  and  $\Lambda_2$  if we use the transverse resonance condition of MTLT<sup>[7,8]</sup>

$$Y_{up} + Y_{dn} = 0 \quad (1)$$

where  $Y_{up}$  and  $Y_{dn}$  represent the input admittances when looking up and down at an arbitrary point on the  $x$ -axis, respectively. As explicitly known at the modal representation of MTLT, the characteristic impedance  $Z_m$  of each segment is then related to the propagation constant  $\kappa_m$  as follows:

$$Z_m = \frac{1}{Y_m} = \begin{cases} \frac{\omega\mu}{\kappa_m} & \text{for TE modes} \\ \frac{\kappa_m}{\omega\epsilon_o\epsilon_m} & \text{for TM modes} \end{cases} \quad (2)$$

with  $m=1, 2$ . Also, the input-output relation between

three transmission-line blocks becomes

$$\begin{pmatrix} V_{out} \\ I_{out} \end{pmatrix} = T_1 T_2 T_1 \begin{pmatrix} V_{in} \\ I_{in} \end{pmatrix}, \quad (3)$$

where  $T_m$  is the transfer matrix of the  $m$ -th block which yields

$$T_m = \begin{bmatrix} \cos(\kappa_m d_m) & iZ_m \sin(\kappa_m d_m) \\ iY_m \sin(\kappa_m d_m) & \cos(\kappa_m d_m) \end{bmatrix}$$

and  $d_m$  is the length of each transmission-line block given by  $d_1 = \Lambda_1/2$ ,  $d_2 = \Lambda_2$ . Then, the symmetric unit-cell network can be expressed by an equivalent network with equivalent propagation constant  $\kappa_{eq}$  satisfying Floquet's theorem, which states the fact that periodic structures have a solution which consists of an exponential factor multiplied by a periodic function of period  $\Lambda$ . Figure 2(c) presents the equivalent network obtained by Floquet's exponential solution with equivalent propagation constant  $\kappa_{eq}$ . Then, the output components are related to the input components as follows:

$$\begin{pmatrix} V_{out} \\ I_{out} \end{pmatrix} = \begin{bmatrix} \exp(i\kappa_{eq}\Lambda) & 0 \\ 0 & \exp(i\kappa_{eq}\Lambda) \end{bmatrix} \begin{pmatrix} V_{in} \\ I_{in} \end{pmatrix}. \quad (4)$$

Accounting for the consistence of Eqs. (3) and (4), we obtain a dispersion relation

$$\begin{aligned} \cos(\kappa_{eq}\Lambda) &= \cos(\kappa_1\Lambda_1)\cos(\kappa_2\Lambda_2) \\ &- \frac{1}{2} \left( \frac{Z_2}{Z_1} + \frac{Z_1}{Z_2} \right) \sin(\kappa_1\Lambda_1)\sin(\kappa_2\Lambda_2). \end{aligned} \quad (5)$$

Consequently, the eigenvalue problem above may be numerically calculated to analyze such optical characteristics as the pass-band filtering or the single mode oscillation of quarter-wavelength phase-shifted DFB guides based on semiconductor materials with gain or loss.

## 2. Equivalent Characteristic Impedance

In previous subsection, we have derived the

propagation constant  $\kappa_{eq}$  of equivalent transmission-line network identifying DFB guiding regions. However, to explore the filtering characteristics of DFB guiding structure, we must define newly the characteristic impedance  $Z_{eq}$  of the equivalent network because the characteristic impedance of periodic guiding structures is not such simply related to the propagation constant as Eq. (2) being supported only at the stratified guiding structures. To implement the equivalent blocks of quarter-wavelength DFB guides, we apply bisection principle (called Babinet's principle) to a symmetric plane of the sectored network shown in Fig 2(b). The bisection principle implies that the fields on the source-free guides of a closed surface are completely determined by stating the values of tangential electric and magnetic fields on either one portion or the remainder of the surface. If a magnetic (or electric) conducting wall for TE (or TM) modes is then placed at the symmetric plane, the bisected equivalent network is terminated by open-bisection or short-bisection dependent on even or odd modes as shown in Fig. 3. This results in the input impedance

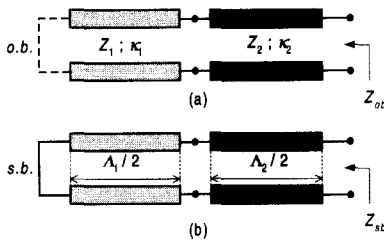


그림 3. Babinet원리를 만족하는 등가전송선로 : (a) 개방 이등분, (b) 단락 이등분

Fig. 3. Network configurations satisfying Babinet's theorem terminated by (a) open-bisection (o.b.), and (b) short-bisection (s.b.).

$$Z_{ob} = iZ_1 \frac{Z_2 - Z_1 \tan\left(\frac{\kappa_1 \Lambda_1}{2}\right) \tan\left(\frac{\kappa_2 \Lambda_2}{2}\right)}{Z_1 \tan\left(\frac{\kappa_2 \Lambda_2}{2}\right) + Z_2 \tan\left(\frac{\kappa_1 \Lambda_1}{2}\right)} \quad (6)$$

for open-bisection, and

$$Z_{sb} = -iZ_1 \frac{Z_1 \tan\left(\frac{\kappa_1 \Lambda_1}{2}\right) + Z_2 \tan\left(\frac{\kappa_2 \Lambda_2}{2}\right)}{Z_1 - Z_2 \tan\left(\frac{\kappa_1 \Lambda_1}{2}\right) \tan\left(\frac{\kappa_2 \Lambda_2}{2}\right)} \quad (7)$$

for short-bisection, where the subscript *ob* and *sb* stand for open-bisection and short-bisection, respectively. Then, the equivalent characteristic impedance for a symmetric unit-cell of DFB guiding regions can be expressed as

$$Z_{eq} = \sqrt{Z_{ob} Z_{sb}} \quad (8)$$

Consequently, the equivalent transmission-line network developed newly by the equivalent propagation constant of Eq. (5) and characteristics impedance of Eq. (8) can systematically serve to analyze the optical properties of DFB guiding structures, as will be discussed in detail below.

### 3. Modal Transmission-Line Equations

As mentioned before, although such some simplified methods as CMT and TMM give us simplicity and convenience like the equivalent network approach proposed in this paper, they have serious disadvantages when analyzing the physical insight of modes propagating along with the multi-sectional periodic guiding structures. On the other hand, our approach is governed by general transmission-line equations whose modal parameters are analogous to the wave equations of uniform electric and magnetic fields incident into DFB guides. Thus, the equivalent network depicted in Fig. 1(b) acts as a quarter-wave impedance transformer, which can characterize completely the design concepts and treat easily in basic electromagnetic theory.

Each equivalent network presenting DFB and phase-shift regions then supports a modal voltage for TE modes, which is expressed as a superposition of exponentially decreasing and increasing traveling-waves along *z*-direction. Assuming that a surface wave with amplitude  $V_{f,0}$  is incident into the input junction terminal  $z=0$ , the modal voltage in the constituent blocks is given by

$$\begin{aligned} V_0(z) &= V_{f,0} \left\{ e^{ik_z z} + \Gamma_0 e^{-ik_z z} \right\} , \\ V_m(z) &= V_{f,m} \left\{ e^{ik_z m(z-h_{m-1})} + \Gamma_m e^{2ik_z m' h} e^{-ik_z m(z-h_{m-1})} \right\} \text{ for } m \neq 0, 4 , \\ V_4(z) &= V_{f,4} e^{ik_z 4(z-h_4)} \end{aligned} \quad (9)$$

from conventional transmission-line theory. Here, the forward-traveling voltage  $V_{f,m}$  is the complex amplitude of modal voltage, and must satisfy the continuity conditions at all  $z=h_m$  boundaries so that we have

$$\begin{aligned} V_{f,0} &= \frac{1 + \Gamma_1 e^{2ik_z h_1}}{1 + \Gamma_0} \\ V_{f,1} &= 1 \\ V_{f,m} &= \frac{V_{f,m-1} e^{2ik_z h_{m-1}} (1 + \Gamma_{m-1})}{1 + \Gamma_m e^{2ik_z h_m}} \quad \text{for } m > 1 \end{aligned}$$

with a convenient normalization for  $V_{f,1}$ . Also, the propagation constants correspond to the equivalent terms as

$$k_{z,m} = \begin{cases} \kappa & \text{for } m = 0, 2, 4 \\ \kappa_{eq} & \text{for } m = 1, 3 \end{cases}$$

As already known well, the reflection coefficients looking to the right at  $z=h_m$  due to the impedance mismatching between the equivalent blocks may be determined by

$$\begin{aligned} \Gamma_m &= \frac{(Y_m - Y_{m+1}) + (Y_m + Y_{m+1})\Gamma_{m+1} e^{2ik_z h_{m+1}}}{(Y_m + Y_{m+1}) + (Y_m - Y_{m+1})\Gamma_{m+1} e^{2ik_z h_{m+1}}} \quad \text{for } m < 4 \\ \Gamma_4 &= \frac{Y_3 - Y_4}{Y_3 + Y_4} \end{aligned} \quad (10)$$

where the characteristic admittances of each transmission-line block stand for

$$Y_m = \begin{cases} 1/Z & \text{for } m = 0, 2, 4 \\ 1/Z_{eq} & \text{for } m = 1, 3 \end{cases}$$

Consequently, we can determine the reflected power

$$P_{ref} = |\Gamma_0|^2 P_{in} \quad (11)$$

for TE modes at input boundary  $z=0$ . Subsequently, using the equations defined above and assuming that the input power  $P_{in}$  is normalized to unity, the power  $P_{tr}$  transmitted through the output boundary  $z=h_3$  becomes

$$P_{tr} = \frac{|V_3(z=h_3)|^2}{Z} = |V_{f,3}(1 + \Gamma_3)e^{ik_z h_3}|^2 \quad (12)$$

Similarly, the reciprocal descriptions for TM modes are obtained by expressing the equations for modal voltages in Eqs. (9)~(12) with those ones for modal currents. In the following numerical discussion, we will discuss only the optical properties of TE modes, but we can extend our approach to evaluate TM modes with no tedious works.

### III. Numerical Results and Discussions

The guiding problems of a quarter-wavelength phase-shifted DFB guide are explicitly and numerically evaluated by applying conventional transmission-line considerations based on the corresponding boundary conditions of Maxwell's equations. As mentioned already, the equivalent network of Fig. 1(b) is analogous to a quarter-wave transformer, being a useful circuit for matching between transmission lines in microwave engineering area. Thus, for simplicity and to emphasize the main aspect of interest here, we will call the quarter-wavelength phase-shifted DFB guide as a quarter-wave transformer throughout this numerical analysis.

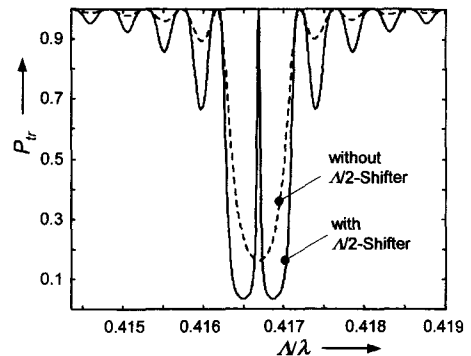


그림 4.  $\lambda/2$  천이영역이 있는 구조와 천이영역이 없는 DFB 구조의 투과전력.

Fig. 4. Calculated transmission of DFB grating with and without  $\lambda/2$  phase-shifter.

As the first step of numerical evaluation, we treat the reflected power given by Eq. (11) at the input boundary when an optical power is incident into a quarter-wave transformer with or without the phase-shifter. Figure 4 shows that the quarter-wave transformer with no shifter and length  $150 \text{ \AA} \mu\text{m}$  has a peak value at  $\Lambda/\lambda = 0.4167$  for fundamental TE mode, as known well. Whereas, the quarter-wave transformer with  $\Lambda/2$ -shifter and length  $t_1 = t_2 = 150 \text{ \AA} \mu\text{m}$  occurs a deep pole at the normalized wavelength, meaning that the pass-band property and a single resonance mode exist.

This phenomenon can be explained by the impedance matching condition of a single-section transformer with narrow pass-band. The characteristic impedance of the matching section of a single-section quarter-wave transformer satisfying the matching condition is

$$Z = \sqrt{Z_{r2}Z_{r1}} \quad (13)$$

where  $Z_{r1}$  and  $Z_{r2}$  represent the input impedance looking to the left at  $z = h_1$  and to the right at  $z = h_2$ , respectively. Then, the matching condition of Eq. (13) holds at the resonance frequency of pass-band filter so that there is no reflection at the input boundary  $z = 0$  of Fig. 1(b). However, the condition is no longer satisfied at the other frequencies and some portions of the incident power reflect due to the impedance

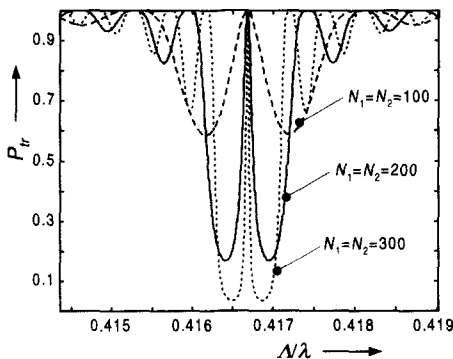


그림 5. 격자수의 변화에 따른 등가전송선로의 투과 전력

Fig. 5. Calculated transmission of the quarter-wave transformer along the variation of grating numbers.

mismatching. Furthermore, this single-section quarter-wave transformer can be simply extended to multi-section geometry and be synthesized to yield a desired frequency bandwidth in optical band-pass filter.

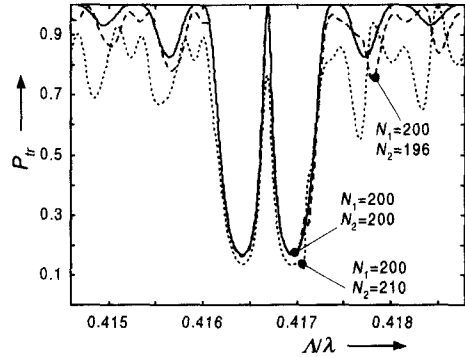


그림 6. 두개의 비대칭격자로 구성된 등가전송선로의 투과전력.

Fig. 6. Calculated transmission of the quarter-wave transformer consisted of two asymmetric DFB gratings.

Next, we examine the variation of transmitted power along the increase of the number of gratings of two DFB guiding blocks. As shown in Fig. 5, as the grating number  $N_1$  and  $N_2$  equally increase, the mismatching values not satisfying the condition of Eq. (13) remarkably increase and it causes the bandwidth of transformer to have narrower pass-band selectivity. Furthermore, we obtain an interesting result by exploring the asymmetric property of the two equivalent blocks. Figure 6 shows that the pass-band filtering characteristics as well as the quality of side-lobes gradually degrade along the increasing amount of the geometrical discrepancy of those guiding structures. Because the condition given in Eq. (13) for impedance match is no longer held at the quarter-wave transformer consisted of two asymmetric DFB gratings.

As stated above, we have analyzed the filtering properties of passive quarter-wave transformer without gain or loss. Now, we consider the oscillating characteristics of active quarter-wave transformer with gain. Then, the refractive index of the guiding layer is a complex value like  $n_j = 3.64 - in_j''$  in which the

imaginary refractive index  $n_f''$  describes the gain component. If the gain overcomes a total loss of quarter-wave transformer chiefly dependent on the radiation loss of modes traveling through two DFB guides, the guided wave propagates without attenuation. We refer to this gain value as the transparency gain, for which the recycling wave inside phase-shifter neither grow nor decay on each round-trip. Consequently, the active device begins constructive oscillation at larger gain values than the transparency gain, and allows one resonance mode to oscillate. The detailed spectrums for various gain values are shown in Fig. 7. This spectral configuration

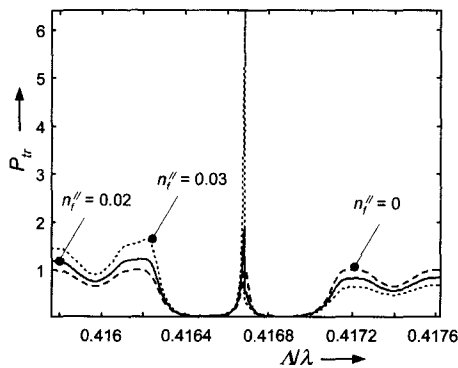


그림 7.  $N_1 = N_2 = 300$ 인 격자로 구성된 등가전송선로의 투과전력에 대한 발진 응답

Fig. 7. Oscillation response for the transmitted power of quarter-wave transformer with the grating number  $N_1 = N_2 = 300$ .

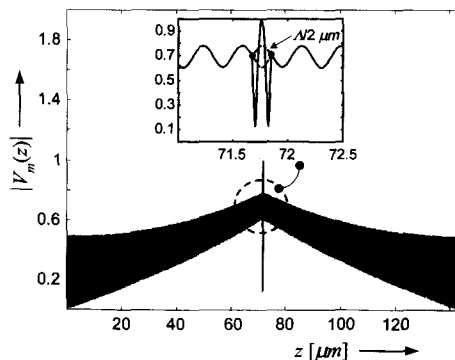


그림 8. 등가전송선로에서 전파하는 정규화된 모드 전압

Fig. 8. Normalized amplitude of modal voltage propagating along the quarter-wave transformer.

gives an excellent illustration describing how a single oscillating mode emerges just above threshold and a deep hole casts just below threshold.

Finally, to understand completely the physical insight of quarter-wave transformer at the resonance condition ( $\lambda/\lambda_0 = 0.4167$ ), we sketch the power normalized by an arbitrary scale as a function of propagating distance in Fig. 8. As shown in the figure, the powers escaping from the interfaces between phase shifter and two DFB gratings exponentially decay, and suffer sinusoidal ripple-beat pattern due to the discontinuity of grating facets. The narrower of the peak in Fig. 8 is further expanded in the insert. The insert shows that the quarter-wavelength shift of the propagating wave occurs at the boundaries between phase-shifter and two DFB gratings rather than at the center of phase-shifter as mentioned in previous works<sup>[9,10]</sup>. Such a behavior is illustrated by sinusoidal dashed-lines in the insert, and it gives a newly presented insight, that is, there exists a distribution of modal voltage confined well within the range of phase-shifter. It is the reason why a single resonance mode oscillates in the quarter-wave transformer with gain. To the best of my knowledge, this is a novel and interesting phenomenon being reported first in this paper. Thus, we need more detailed analysis for the modal voltage distributing along the distance of quarter-wave transformer with gain or loss. However, we do not present the detailed discussion in this paper because it is beyond the scope of this paper. Later we will report those results as a paper.

#### IV. Conclusions

In this paper, we have presented a newly developed analytic approach to evaluate easily and explicitly the filtering and oscillating characteristics of a quarter-wavelength phase-shifted DFB guiding structures. The equivalent network approach is based on Floquet's theorem and Babinet's principle used widely in the design and analysis of devices in microwave engineering field. Furthermore, it does not need to run

tedious numerical programs when solving the complicated eigenvalue problems of the multi-layered and multi-sectioned DFB guides. Consequently, these overall results reveal that the extended modal transmission-line theory is served as a convenient and powerful analytic algorithm for the design and analysis of planar DFB guiding structures in optical communication, even no matter whether it contains materials with gain or loss.

### 참 고 문 헌

- [1] H. Kogelnik and C. V. Shank, "Coupled-Wave Theory of Distributed Feedback Lasers," *J. App. Phys.*, Vol. 43, pp. 2327~2335, May 1972.
- [2] H. A. Haus and Y. Lai, "Theory of Cascaded Quarter Wave Shifted Distributed Feedback Resonators," *IEEE J. Quantum Electron.* Vol. 28, pp. 205-213, 1992.
- [3] R. Kashyap, *Fiber Bragg Gratings*, pp. 179-185, Academic Press, 1999.
- [4] L. Felsen and N. Marcuvitz, *Radiation and Scattering of Waves*, pp. 183-215, IEEE Press, 1973.
- [5] W. L. Weeks, *Electromagnetic Theory for Engineering Applications*, pp. 167-173, John Wiley & Sons, Inc, 1963.
- [6] J. A. Kong, *Electromagnetic Wave Theory*, pp. 373-382, John Wiley & Sons, Inc, 1990.
- [7] K. C. Ho, G. Griffel, T. Tamir, "Polarization Splitting in Lossy/Gainy MQW Directional Couplers," *IEEE J. Lightwave Technol.* Vol. 15, pp. 1233-1240, 1997.
- [8] J. H. Kim, K. C. Ho, Y. K. Kim, H. Y. Lee, H. D. Yoon, "A Novel Approach of Planar DFB Guiding Structures for Optical Communication," *SK Telecom Review* Vol. 9, No. 4, pp. 662-675, 1999.
- [9] Yariv, *Optical Electronics*, pp. 500~511, Saunders College Publishing, 1991.
- [10] H. A. Haus, *Waves and Fields in Optoelectronics*, pp. 243-249, Prentice Hall, 1984.

---

### 저 자 소 개

金 俊 煥(正會員) 電子工學會論文誌 第35卷 D編 7號 參照

扈 光 春(正會員) 電子工學會論文誌 第36卷 D編 11號 參照